Journal of ELECTRONIC MATERIALS, Vol. 40, No. 5, 2011
DOI: 10.1007/s11664-010-1479-7

Effect of Vacancy Distribution on the Thermal Conductivity of Ga_2Te_3 and Ga_2Se_3

CHANG-EUN KIM,[1] KEN KUROSAKI,[1,4] MANABU ISHIMARU,[2] HIROAKI MUTA,[1] and SHINSUKE YAMANAKA[1,3]

1.—Graduate School of Engineering, Osaka University, Suita, Osaka 565-0871, Japan. 2.—Institute of Scientific and Industrial Research, Osaka University, Ibaraki, Osaka 567-0047, Japan. 3.—Research Institute of Nuclear Engineering, University of Fukui, Fukui 910-8507, Japan. 4.—e-mail: kurosaki@see.eng.osaka-u.ac.jp

Our group has focused attention on Ga_2Te_3 as a natural nanostructured thermoelectric material. Ga_2Te_3 has basically a zincblende structure, but one-third of the Ga sites are structural vacancies due to the valence mismatch between Ga and Te. It has been confirmed that (1) vacancies in Ga_2Te_3 exist as two-dimensional (2D) vacancy planes, and (2) Ga_2Te_3 exhibits an unexpectedly low thermal conductivity (κ), most likely due to highly effective phonon scattering by the 2D vacancy planes. However, the effect of the size and periodicity of the 2D vacancy planes on κ has been unclear. In addition, it has also been unclear whether only the 2D vacancy planes reduce κ or if point-type vacancies can also reduce κ. In the present study, we tried to prepare Ga_2Te_3 and Ga_2Se_3 with various vacancy distributions by controlling annealing conditions. The atomic structures of the samples were characterized by means of transmission electron microscopy, and κ was evaluated from the thermal diffusivity measured by the laser flash method. The effects of vacancy distributions on κ of Ga_2Te_3 and Ga_2Se_3 are discussed.

Key words: Thermoelectric, thermal conductivity, structural vacancy, gallium telluride, gallium selenide

INTRODUCTION

Thermoelectric (TE) energy is utilized in power-generation devices that are designed to convert waste heat into electrical energy.[1] The efficiency of such devices is linked to the TE properties of the generator materials and the temperature gradient across the device. The effectiveness of a TE material is determined by the dimensionless figure of merit, $ZT = S^2\sigma T/\kappa$, where S is the Seebeck coefficient, σ is the electrical conductivity, T is the absolute temperature, and κ is the total thermal conductivity. The most important issue in TE research is identifying materials with high ZT, namely with low κ as well as large S with moderate σ. The best TE materials currently used in cooling devices are Bi_2Te_3-based alloys, with a maximum ZT of around 1. $ZT = 1$, which translates to a device efficiency of several percent, was a practical upper limit for bulk materials established in the 1960s.

Since S, σ, and κ in bulk materials are interrelated, it is very difficult to control them independently to increase ZT. However, the assumption is that, if numerous nanoscale interfaces can be introduced, they would scatter phonons more efficiently than electrons, leading to a significant reduction of κ without prejudice to S and σ.[2–4] There have been a few previous studies aimed at establishing proof of principle of this concept; for example, Venkatasubramanian et al.[5] performed TE characterizations of Bi_2Te_3/Sb_2Te_3 superlattices. They demonstrated that the scattering of phonons by the interfaces reduced κ more than σ, leading to the achievement of $ZT > 2$. While ZT has reached high values in such superlattice structures, these

(Received May 15, 2010; accepted December 2, 2010; published online January 4, 2011)

materials are unlikely candidates for practical use. The goal is to achieve similarly high ZT in bulk materials that can be developed in large quantities with lower manufacturing complexity and cost. Kanatzidis et al.[6] reported the exceptionally high ZT (>1.5) of PbTe-based bulk materials due to the very low κ, possibly arising from the compositional modulations on the single nanometer scale, similar to that found in superlattices. However, this is just one way to realize high ZT with bulk-nanostructured materials.

Against this background, we focused attention on Ga_2Te_3 and Ga_2Se_3 as examples of bulk-nanostructured materials. It is well known that Ga_2Te_3 and Ga_2Se_3 have the same crystal structure: a defect zincblende cubic crystal (space group F-43m). Due to the valence mismatch between the cation and anion, one-third of the cation sites are structural vacancies in both Ga_2Te_3 and Ga_2Se_3; i.e., the chemical formula of Ga_2M_3 (M = Te or Se) can be written as $Ga_2VA_1M_3$, where VA denotes a vacancy. Recently, by forming such vacancies in the crystal, a significant reduction in the lattice thermal conductivity due to strong phonon–vacancy scattering was observed in InSb-In_2Te_3 solid solutions.[7] It has been expected that Ga_2Te_3 and Ga_2Se_3 have a mesoscopic superstructured phase, having vacancy planes.[8,9] In our previous studies,[10,11] the existence of regularly arranged two-dimensional (2D) vacancy planes with approximately 10 lattice (equivalent to 3.5 nm) intervals was confirmed in Ga_2Te_3.[10] Furthermore, in solid solutions of $(Ga,In)_2Te_3$, such vacancy planes also existed, but the periodicity of the intervals was random.[11] We hypothesized that, if we could create such vacancy planes in bulk Ga_2Te_3 and Ga_2Se_3 and control their size and periodicity, we could achieve low κ, due to the effective phonon scattering by the vacancy planes.

In the present study, we tried to control the vacancy distribution in Ga_2Te_3 and Ga_2Se_3 by changing the annealing conditions. We succeeded in preparing the following four bulk materials:

1. Ga_2Te_3 with randomly arranged vacancy planes
2. Ga_2Te_3 with regularly arranged vacancy planes (approximately 3.5 nm interval)
3. Ga_2Se_3 with ordered vacancies as a point defect
4. Ga_2Se_3 with randomly arranged vacancy planes

By characterizing these four materials, the effects of vacancy distribution on κ of Ga_2Te_3 and Ga_2Se_3 were studied.

EXPERIMENTAL PROCEDURES

Ga_2Te_3 and Ga_2Se_3 pieces were sealed in silica tubes and melted at 1273 K overnight. The melted and cooled samples were crushed to fine powders, followed by hot-pressing at 873 K for 3 h under a pressure of 62 MPa in an argon flow atmosphere. After hot-pressing, the obtained pellets were annealed under appropriate conditions to obtain the samples with various vacancy distributions. The annealing conditions are summarized in Tables I and II for Ga_2Te_3 and Ga_2Se_3, respectively. To characterize the crystallographic properties of the samples, we collected powder x-ray diffraction (XRD) data using a diffractometer (RINT2000, RIGAKU) with Cu K_α radiation in air at room temperature.

κ was evaluated using the expression $\kappa = \alpha C_p d$, where α is the thermal diffusivity, C_p is the specific heat capacity, and d is the density. α was measured under vacuum using a laser flash apparatus in the temperature range from room temperature to 700 K to 750 K. C_p was estimated from the Dulong–Petit model, $C_p = 3nR$, where n is the number of atoms

Table I. Annealing conditions and vacancy distributions of the Ga_2Te_3 samples

Sample Name	GT–LT (Ga_2Te_3 Annealed at Low Temperature)	GT–HT (Ga_2Te_3 Annealed at High Temperature)
Annealing temperature (K)	673	973
Annealing period (days)	14	14
Cooling method	Furnace cool	Quench
Vacancy distribution	In-plane type with random periodicity	In-plane type with regular periodicity (approximately 3.5 nm interval)

Table II. Annealing conditions and vacancy distributions of the Ga_2Se_3 samples

Sample Name	GS–LT (Ga_2Se_3 Annealed at Low Temperature)	GS–HT (Ga_2Se_3 Annealed at High Temperature)
Annealing temperature (K)	873	1173
Annealing period (days)	30	7
Cooling method	Quench	Quench
Vacancy distribution	Point type	In-plane type with random periodicity

per formula unit and R is the gas constant. Note that the Dulong–Petit model is not a sufficiently accurate measure of C_p. In fact, the value of the Dulong–Petit limit for C_p for Ga_2Te_3 is $15R$ = 124.7 J K^{-1} mol^{-1}, whereas the literature value of C_p (298.15 K) for Ga_2Te_3 measured by using an adiabatic calorimeter is 119.21 J K^{-1} mol^{-1}.[12] The densities of the hot-pressed samples calculated based on the measured weights and dimensions were above 96% of the theoretical densities.

Transmission electron microscopy (TEM) observations were performed using a JEOL JEM-3000F with an incident electron energy of 300 kV. Flakes of single crystals, obtained by crushing the pellets, were used for TEM samples. High-resolution TEM images and diffraction patterns were recorded on imaging plates.

RESULTS AND DISCUSSION

Effect of Periodicity of the Two-Dimensional Vacancy Planes on the Thermal Conductivity of Ga_2Te_3[13]

As summarized in Table I, two kinds of Ga_2Te_3 samples were prepared: the sample annealed at 673 K for 14 days and then furnace cooled (GT–LT: Ga_2Te_3 annealed at low temperature), and the sample annealed at 973 K for 14 days and then water quenched (GT–HT: Ga_2Te_3 annealed at high temperature). Figure 1 shows powder XRD patterns of the GT–LT and the GT–HT samples. Basically, all the peaks for both samples could be indexed to the zincblende structure. In the XRD pattern of the GT–HT sample, a few peaks were observed before and after the (111) peak, suggesting that the vacancy may concentrate on the (111) plane. On the other hand, in the XRD pattern of the GT–LT sample, such satellite peaks exist but broaden. This peak broadening is closely related with the periodicity of the vacancy planes.

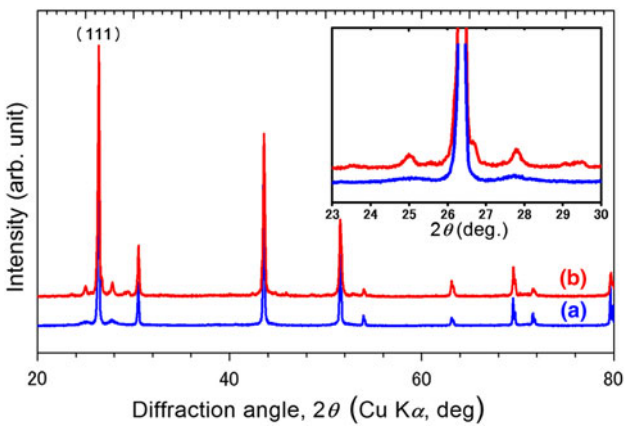

Fig. 1. (Color online) Powder XRD patterns of the Ga_2Te_3 samples: (a) GT–LT: Ga_2Te_3 annealed at low temperature, and (b) GT–HT: Ga_2Te_3 annealed at high temperature.

Figure 2 shows high-resolution TEM images and electron diffraction patterns taken from a single grain of a sintered pellet of Ga_2Te_3 annealed under different conditions. These micrographs were obtained with the electron beam aligned along the $[1\bar{1}0]$ direction. In the high-resolution TEM image of the GT–HT sample (Fig. 2b), plane defects due to the vacancy-rich plane are two-dimensionally arranged throughout the whole area of the sample. These plane defects appear at the (111) plane with approximately 10 lattice (equivalent to 3.5 nm) intervals. Similar two-dimensional (2D) vacancy planes are also observed in the GT–LT sample, but their periodicity is random (Fig. 2a). These high-resolution TEM results are well consistent with both the electron diffraction and the XRD patterns; that is, in the electron diffraction pattern of the GT–HT sample, superlattice spots exist at the ~1/10 positions between two neighboring fundamental spots along the [111] direction, in addition to the fundamental Bragg reflections due to the zincblende structure. Meanwhile, in the electron diffraction pattern of the GT–LT sample, the superlattice reflections are diffuse and a streak can be seen. Also, a broadening of the satellite peaks can be seen in the XRD pattern of the GT–LT sample (Fig. 1), which is most likely due to the random periodicity of the 2D vacancy planes.

Figure 3 shows the temperature dependence of κ of the samples of Ga_2Te_3 annealed under different conditions. Generally, κ is given by the sum of the electronic and lattice thermal contributions, i.e., $\kappa = \kappa_{el} + \kappa_{lat}$, where κ_{el} and κ_{lat} are the electronic and lattice contributions, respectively. κ_{el} can be roughly calculated using the Wiedemann–Franz relation with the Lorenz number (L), i.e., $\kappa_{el} = L\sigma T$. In the present study, we assumed that the measured κ corresponds to κ_{lat}, because Ga_2Te_3 exhibits quite low σ values, e.g., 0.42 Ω^{-1} m^{-1} at 338 K.[10] By using the value of $L = 2.45 \times 10^{-8}$ W Ω K^{-2}, κ_{el} at 338 K was calculated to be 3.5×10^{-6} W m^{-1} K^{-1}, which can be considered to be zero. As shown in Fig. 3, the κ values of both samples are exceptionally low, i.e., around 0.5 W $m^{-1}K^{-1}$, indicating the possible presence of highly effective phonon scattering due to the 2D vacancy plane structures. On the other hand, there is little difference between the κ values of the GT–LT and GT–HT samples. This means that the presence of the 2D vacancy planes is predominant in achieving the significant reduction of κ, while the periodicity of the vacancy planes has little effect on κ.

Effect of Vacancy Distribution on the Thermal Conductivity of Ga_2Se_3

As summarized in Table II, two kinds of Ga_2Se_3 samples were prepared: the sample annealed at 873 K for 30 days and then water quenched (GS–LT: Ga_2Se_3 annealed at low temperature), and the sample annealed at 1173 K for 7 days and then

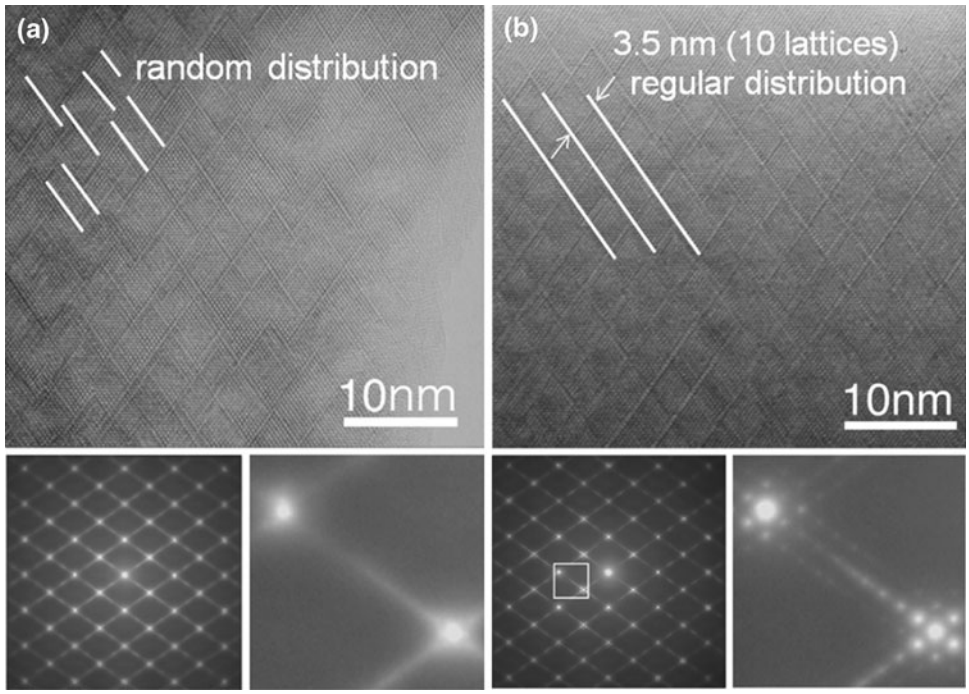

Fig. 2. High-resolution TEM images and electron diffraction patterns of the Ga_2Te_3 samples: (a) GT–LT: Ga_2Te_3 annealed at low temperature, and (b) GT–HT: Ga_2Te_3 annealed at high temperature.

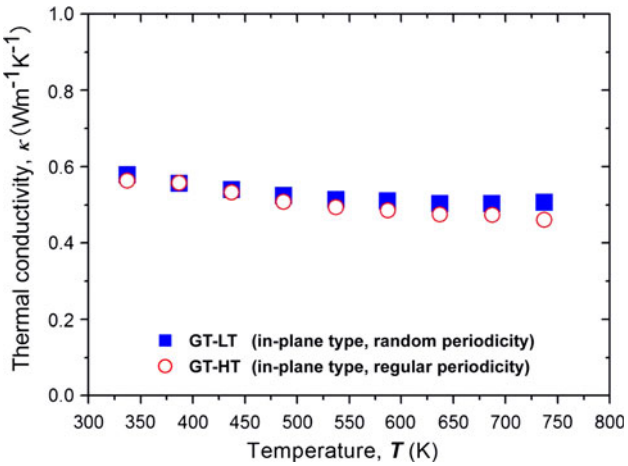

Fig. 3. (Color online) Temperature dependence of the thermal conductivity (κ) of the Ga_2Te_3 samples. Solid squares represent GT–LT: Ga_2Te_3 annealed at low temperature (in-plane-type vacancies with random periodicity); open circles represent GT–HT: Ga_2Te_3 annealed at high temperature (in-plane-type vacancies with regular periodicity).

water quenched (GS–HT: Ga_2Se_3 annealed at high temperature). Figure 4 shows powder XRD patterns of the GS–LT and GS–HT samples. Basically, all the peaks for both samples could be indexed to the zincblende structure, as observed for Ga_2Te_3 (Fig. 1). In the XRD pattern of the GS–LT sample, very sharp peaks are observed. On the other hand, in the XRD pattern of the GS–HT sample, the peaks broaden and the intensity of the (111) peak significantly weakens, suggesting that the 2D vacancy planes exist along the [111] direction.

Figure 5 shows high-resolution TEM images and electron diffraction patterns taken from a single grain of a sintered pellet of Ga_2Se_3 annealed under different conditions. The diffraction pattern of Fig. 5a is consistent with the (001) reciprocal lattice plane of Ga_2Se_3 [space group: Cc (no. 9), a = 0.6608 nm, b = 1.16516 nm, c = 0.66491 nm, α = 90°, β = 108.84°, γ = 90°] in which vacancies induced by the valence mismatch between the cation and anion are regularly arranged on the Ga sublattice.[14] The high-resolution TEM image of Fig. 5a shows that no vacancy planes are formed, indicating that the vacancies in the GS–LT sample exist as a point defect. On the other hand, in the high-resolution TEM image of the GS–HT sample (Fig. 5b), there exist 2D vacancy planes at the (111) plane with random periodicity, similar to the GT–LT sample (Fig. 2a). In addition, a streak between the fundamental Bragg reflections due to the zincblende structure can be observed in the electron diffraction pattern of the GS–HT sample. We succeeded in preparing two kinds of vacancy distributions in Ga_2Se_3; one includes 2D vacancy planes and the other contains vacancies as a point defect.

Figure 6 shows the temperature dependence of κ of the samples of Ga_2Se_3 annealed under different conditions. Apparently, the κ values of the GS–LT sample with point-type vacancies are higher than those of the GS–HT sample with in-plane-type vacancies. In addition, different behavior is observed in the temperature dependence of κ between the GS–LT and the GS–HT samples; that is, κ of the GS–LT sample with point-type vacancies

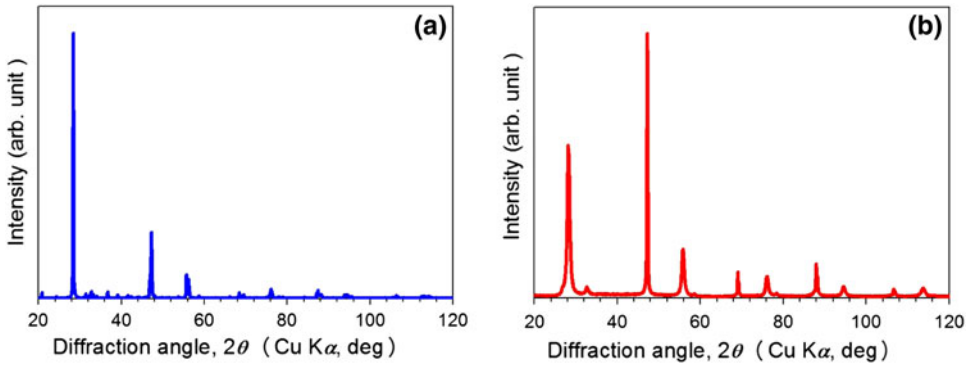

Fig. 4. (Color online) Powder XRD patterns of the Ga_2Se_3 samples: (a) GS–LT: Ga_2Se_3 annealed at low temperature, and (b) GS–HT: Ga_2Se_3 annealed at high temperature.

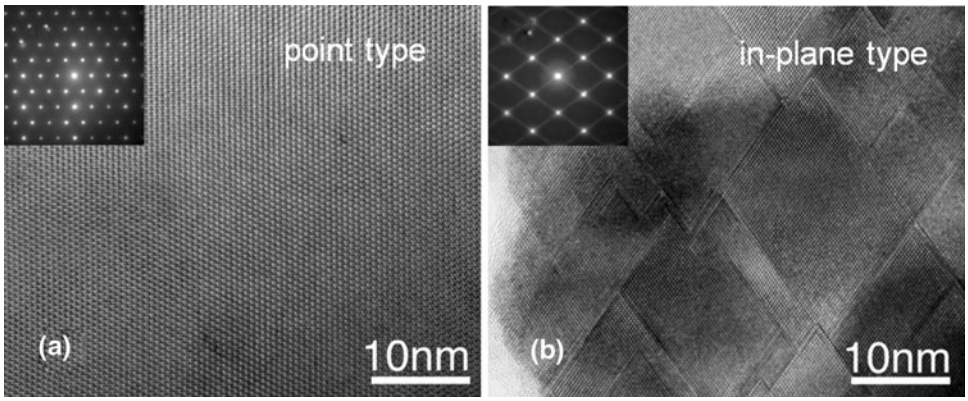

Fig. 5. High-resolution TEM images and electron diffraction patterns of the Ga_2Se_3 samples: (a) GS–LT: Ga_2Se_3 annealed at low temperature, and (b) GS–HT: Ga_2Se_3 annealed at high temperature.

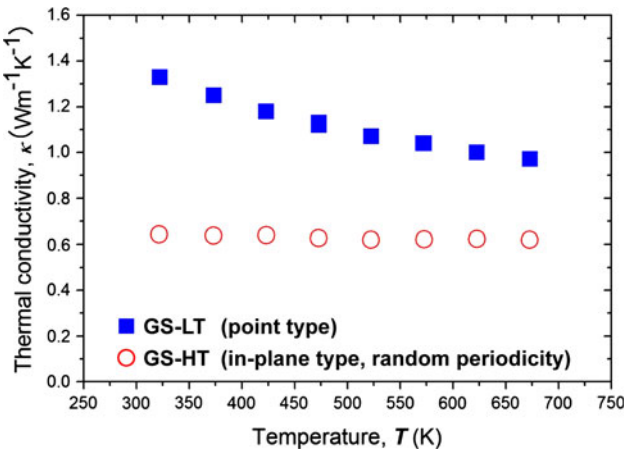

Fig. 6. (Color online) Temperature dependence of the thermal conductivity (κ) of the Ga_2Se_3 samples. Solid squares represent GS–LT: Ga_2Se_3 annealed at low temperature (point-type vacancies); open circles represent GS–HT: Ga_2Se_3 annealed at high temperature (in-plane-type vacancies with random periodicity).

decreases with increasing temperature roughly according to a T^{-1} relation, while that of the GS–HT sample with in-plane-type vacancies exhibits a rather flat temperature dependence. From these results, it can be concluded that phonons are scattered more effectively by the vacancies when they exist as an in-plane-type defect than when they distribute as a point-type defect.

CONCLUSIONS

In the present study, dense polycrystalline samples of Ga_2Te_3 and Ga_2Se_3 with various vacancy distributions were prepared and their κ evaluated. In the case of Ga_2Te_3, the existence of 2D vacancy planes was confirmed. We succeeded in preparing two kinds of bulk Ga_2Te_3 samples by changing the annealing conditions: one with randomly arranged vacancy planes and the other with regularly arranged vacancy planes (3.5 nm interval). Both samples exhibited an unexpectedly low κ with a rather flat temperature dependence, which is most likely due to highly effective phonon scattering by the vacancy planes. However, there was little difference between the κ values of the samples with different distributions of vacancy planes.

On the other hand, in the case of Ga_2Se_3, we succeeded in preparing two kinds of bulk samples; one includes 2D vacancy planes and the other contains vacancies as a point defect. Although these two samples have the same structure with the same

chemical composition and the same vacancy density, their κ values were quite different. The sample with point-type vacancies exhibited a relatively high κ with a T^{-1} temperature dependence, while the sample with in-plane-type vacancies exhibited quite a low κ with a rather flat temperature dependence.

From these experimental results, it was concluded that:

1. Just the presence of vacancies does not lead to effective phonon scattering;
2. Vacancies should form an in-plane-type defect structure to achieve effective phonon scattering;
3. The periodicity of the vacancy planes (i.e., regular or random) has little effect on phonon scattering.

We believe that the introduction of structural vacancies with in-plane-type defect structures is a new method to decrease κ of TE materials, possibly resulting in increased ZT.

ACKNOWLEDGMENTS

This work was supported in part by a Grant-in-Aid for Scientific Research (No. 21760519) from the Ministry of Education, Culture, Sports, Science, and Technology of Japan. Additional support was kindly provided by the Wakasa Wan Energy Research Centre, The Thermal & Electric Energy Technology Foundation, the Association for the Progress of New Chemistry, KRI Inc., and the Murata Science Foundation.

REFERENCES

1. T.M. Tritt and M.A. Subramanian, *Mater. Res. Soc. Bull.* 31, 188 (2006).
2. L.D. Hicks and M.S. Dresselhaus, *Phys. Rev. B* 47, 12727 (1993).
3. L.D. Hicks, T.C. Harman, X. Sun, and M.S. Dresselhaus, *Phys. Rev. B* 53, R10493 (1996).
4. M.S. Dresselhaus, G. Chen, M.Y. Tang, R.G. Yang, H. Lee, D.Z. Wang, Z.F. Ren, J-.P. Fleurial, and P. Gogna, *Adv. Mater.* 19, 1043 (2007).
5. R. Venkatasubramanian, E. Siivola, T. Colpitts, and B. O'Quinn, *Nature* 413, 597 (2001).
6. K.F. Hsu, S. Loo, F. Guo, W. Chen, J.S. Dyck, C. Uher, T. Hogan, E.K. Polychroniadis, and M.G. Kanatzidis, *Science* 303, 818 (2004).
7. Y. Pei and D.T. Morelli, *Appl. Phys. Lett.* 94, 122112 (2009).
8. M.M. Guymont, A. Tomas, and M. Guittard, *Philos. Mag. A* 66, 133 (1992).
9. N. Teraguchi, F. Kato, M. Konagai, K. Takahashi, Y. Nakamura, and N. Otsuka, *Appl. Phys. Lett.* 59, 567 (1991).
10. K. Kurosaki, H. Matsumoto, A. Charoenphakdee, S. Yamanaka, M. Ishimaru, and Y. Hirotsu, *Appl. Phys. Lett.* 93, 012101 (2008).
11. S. Yamanaka, M. Ishimaru, A. Charoenphakdee, H. Matsumoto, and K. Kurosaki, *J. Electron. Mater.* 38, 1392 (2009).
12. A.V. Tyurin, K.S. Gavrichev, V.P. Zlomanov, and N.N. Smirnova, *Inorg. Mater.* 42, 855 (2006).
13. C.E. Kim, K. Kurosaki, M. Ishimaru, D.Y. Jung, H. Muta, and S. Yamanaka, *Phys. Status Solidi RRL* 3, 221 (2009).
14. P. Villars and L D. Calvert, *Peason's Handbook of Crystallographic Data for Intermetallic Phases*, Vol. 3 (Metals Park: American Society for Metals, 1985).